Transport hysteresis and zonal flow stimulation in magnetized plasmas

Etienne Gravier, Maxime Lesur, Thierry Réveillé, T. Drouot, J. Médina

Transport hysteresis and zonal flow stimulation in magnetized plasmas

E. Gravier,* M. Lesur, T. Reveille, T. Drouot, and J. Médina

Institut Jean Lamour, UMR 7198 CNRS - Université de Lorraine, 54 500 Vandoeuvre-lès-Nancy

(Dated: 23 août 2017)

Résumé

A hysteresis in the relationship between zonal flows and electron heating is observed numerically by using gyrokinetic simulations in fusion plasmas. As the electron temperature increases, a first transition occurs, at a given electron/ion temperature ratio, above which zonal flows are much weaker than before the transition, leading to a poorly confined plasma. Beyond this transition, even if the electron temperature is lowered to a moderate value, the plasma fails to recover a dynamic state with strong zonal flows. Then, as the electron temperature decreases further, a new transition appears, at a temperature lower than the first transition, below which the zonal flows are stronger than they were initially. The confinement of the plasma and the heat flux are thus found to be sensitive to the history of the magnetized plasma. These transitions are associated with large exchanges of energy between the modes corresponding to instabilities ($m > 0$) and zonal flows ($m = 0$). We also observe that up to the first transition it is possible to use a control method to stimulate the appearance of zonal flows and therefore the confinement of the plasma. Beyond that transition, this control method is no longer effective.

* Etienne.Gravier@univ-lorraine.fr

a. Introduction. Zonal flows have attracted the attention of many scientists because of their potential to reduce heat transport [1–6]. They play an important role in regulating turbulence and thus improve the energy confinement of magnetized plasmas. Zonal flows are cells in the poloidal direction which are consistently generated by drift wave turbulence through non linear $E \times B$ coupling. Streamers, in contrast, are radially elongated convective cells which dramatically increase radial heat transport in fusion devices [7]. Several fundamental aspects of zonal flows and streamers remain to be fully explored. The mechanisms underlying the onset and disappearance of these structures are still a subject of discussion [8]. In particular the interplay between zonal flows and turbulence remains a challenging problem in tokamak physics [9]. Moreover, there is a great deal of interest in enhancing strong and robust zonal flows in magnetized plasmas.

To uncover underlying mechanisms, we use a gyrokinetic code which only takes trapped particles into account. The turbulence driven by trapped particles (Trapped Electron Mode - TEM and Trapped Ion Mode - TIM) is characterized by frequencies of the order of a slow trapped particle precession frequency. Studying the dynamics at this time scale is therefore relevant for the analysis of TEM and TIM turbulence properties. This model also stands as a prototype for more general turbulence including higher frequency turbulences driven by the kinetics of passing particles. Focusing on kinetic trapped particles (with adiabatic passing particles) makes it possible to average the kinetic equation over the cyclotron and the bounce motions, and allows the number of independent variables in phase-space to be reduced. The gyro-bounce average filters the fast frequencies ω_c (cyclotron frequency) and ω_b (bounce frequency) as well as the small space scales ρ_c (Larmor radius) and δ_b (banana width). It reduces the dimensionality of the model from 6D to 4D [10–14].

This model is developed in action-angle formalism, which means kinetic Vlasov equations are much easier to solve. Only two kinetic variables appear in the differential operators. The other two variables appear as parameters - two adiabatic invariants, namely particle kinetic energy E and the trapping parameter $\kappa = \sqrt{\frac{1-\lambda}{2\varepsilon\lambda}}$, with $\lambda = \mu B_{min}/E$, μ the magnetic moment, B_{min} the minimum magnetic field amplitude, and $\varepsilon = \frac{a}{R_0}$ the inverse of the aspect ratio of the tokamak. Thus the final model involves two parameters (E, κ) and the 2D space coordinates (ψ,α). We consider a tokamak equilibrium with circular concentric magnetic surfaces. The coordinate ψ is the poloidal magnetic flux normalized to the system radial size and stands for the radial coordinate. The quantity α is equal to $\varphi - q\theta$, where θ and φ are

respectively poloidal and toroidal angular coordinates and q is the safety factor defined by $q(\psi) = (\mathbf{B}.\nabla\varphi)/(\mathbf{B}.\nabla\theta)$.

Trapped kinetic electrons have been recently implemented in our model [14–16] and now the code TERESA-4D (Trapped Element REduction in Semi Lagrangian [17] Approach) is capable of covering both TIM/TEM regimes simultaneously. Only trapped particles are kinetic, both passing ions and passing electrons are adiabatic, and the model is collisionless. Therefore neither trapping and de-trapping processes due to turbulent/collisional pitch angle scattering, nor neoclassical physics are taken into account. We observe that zonal flows can transiently appear after the nonlinear phase of saturation of TEM or TIM micro-instabilities depending on the temperature ratio T_e/T_i. In a tokamak, this ratio can be changed for instance by using electron cyclotron resonance heating which leads to different confinement regimes.

Several observations of a hysteresis in the modulation electron cyclotron heating experiments have been reported, for instance on DIII-D plasma [18] or on Large Helical Device (LHD) [19, 20]. Sharp and fast changes of heat flux at the switch-on and switch-off of heating have been reported which has lead to the explained hypothesis that the heating power has an immediate influence on turbulent plasma transport even without a change of mean parameters or mean distribution function.

Moreover, depending on the temperature ratio, magnetically confined plasma may spontaneously exhibit a transition from a low confinement (L-mode) to a high confinement (H-mode) state. The high confinement mode was discovered by the ASDEX team [21], and is the consequence of a self-organizing process in the plasma that is not yet fully understood. Simplified models have been used in order to explain the transition mechanism from the low to high confinement mode in tokamaks. These simplified models exhibit hysteresis, using for instance three equations coupling the drift wave turbulence level, zonal flow speed, and the pressure gradient[22].

Finally, L-H transition has been reported very recently [23] by means of gyrokinetic simulations of edge turbulence in fusion plasmas, leading to the formation of an edge transport barrier just inside the last closed magnetic flux surface.

In this article, we report on our observation of a hysteresis in the relation between zonal flows and electron temperature. This was achieved by using first-principles-based gyrokinetic simulations for core fusion plasmas.

b. Transport hysteresis. In the work described in this paper we vary the temperature ratio $\beta = T_e/T_i$ according to Fig.1 and measure its impact on the energy of zonal flows and drift mode instabilities. In a previous paper [16] we experimented with three ways to act on the ratio T_e/T_i : 1. Modifying the C_{ad} coefficient (see Eq.1 in [16]), which is a function of the temperature ratio, or 2. Modifying the electron temperature of the thermal bath in the core side, or 3. Modifying the electron temperature of the thermal bath in the edge side. We have observed that the efficiency of the modification is not very sensitive to the applied method, or to a combination of the different methods. Whatever the method used, the trends observed are the same. In this paper we focused on the first method (modification of the C_{ad} coefficient). Using this method means that we model a uniform heating rather than a heating energy deposited at selected locations that tailors the temperature profile in the plasma. All other parameters are the same as in [16]. The code is global and full-f, and using these parameters we get $\rho^* = \rho_s/a = 3.0 \times 10^{-2}$, with a the small radius. Time is normalized to the frequency $\omega_0 = T_0/(eR_0^2 B_\theta)$ which corresponds to the ion precession frequency at the typical temperature T_0. In our simulations $T_i = T_0 = 1$, therefore ω_0 is the ion precession frequency. The frequency of trapped modes (TEM and TIM) is of the order of ω_0, and $\omega_c \gg \omega_b \gg \omega_0$, with ω_b the bounce frequency and ω_c the cyclotron frequency.

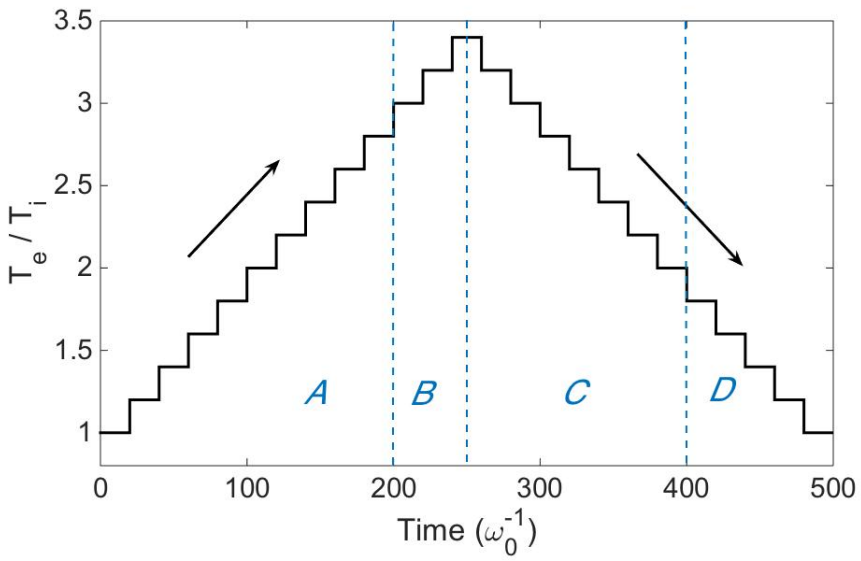

FIGURE 1. Starting from $T_e = T_i$ ($\beta = 1.0$), we gradually increase the electron temperature up to $\beta = 3.4$ and then decrease it back to its initial value $\beta = 1.0$. The time interval between each step is taken sufficiently long (20 ω_0^{-1}) for a steady state to be obtained.

This can be interpreted as a crude model for the following experimental scenario : an increase followed by a decrease in ECRH (Electron Cyclotron Resonance Heating). ECRH is used in many tokamaks - the ITER Tokamak will rely on ECRH heating - and is also for instance the main heating system of Wendelstein 7-X, capable of operating continuously. We stopped our simulations at $T_e/T_i = 3.4$, which is an arbitrary, but reasonable value, given the typical temperature ratios obtained in most modern tokamak experiments with ECRH heating.

To quantify the strength of zonal flows and drift instabilities (TIM and TEM) provided by numerical simulations performed with TERESA, we define the energy contained in the zonal flow,

$$W_{ZF} = \int_0^1 \left\langle \frac{\partial \phi}{\partial \psi} \right\rangle_\alpha^2 d\psi, \tag{1}$$

and the energy contained in drift instability modes,

$$W_{m>0} = \int_0^1 \left\langle \left(\frac{\partial \phi}{\partial \psi} - \left\langle \frac{\partial \phi}{\partial \psi} \right\rangle_\alpha \right)^2 \right\rangle_\alpha d\psi. \tag{2}$$

Here ϕ is the electrostatic potential, $< . >_\alpha$ means average over α, and m is the mode number along the α direction.

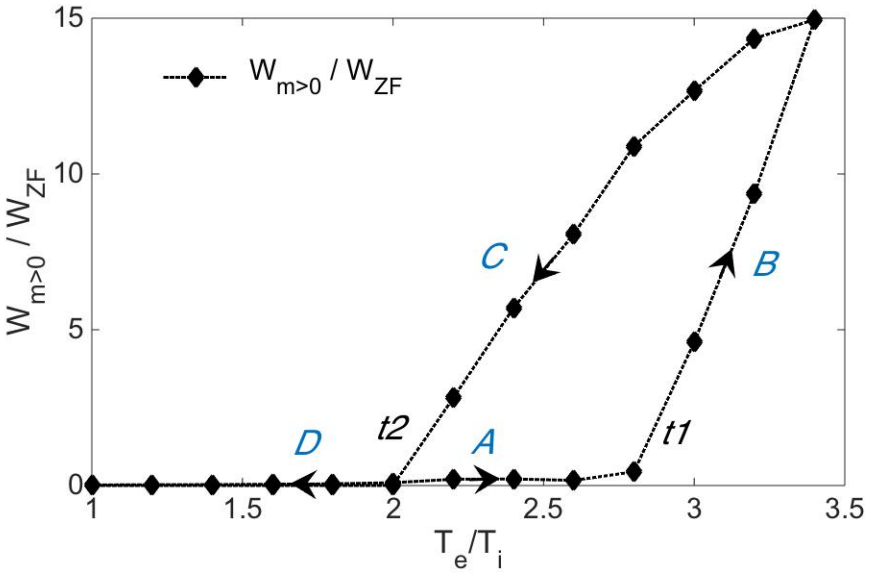

FIGURE 2. $W_{ZF}/W_{m>0}$ plotted against T_e/T_i. The time evolution of T_e/T_i is imposed according to Fig.1. The arrows indicate the path of the hysteresis. Transitions $t1$ and $t2$ are discussed hereafter.

In Fig.2 the ratio $W_{ZF}/W_{m>0}$ is plotted against the temperature ratio T_e/T_i, whose

evolution in time is imposed as depicted in Fig.1. The arrows indicate increasing time. At the beginning (A), from $T_e/T_i = 1$ to 2.8, we observe strong zonal flows which means that the plasma is well confined and the heat transport is low. Then a transition (see $t1$ in Fig.2) occurs between $T_e/T_i = 2.8$ and $T_e/T_i = 3$. The energy contained in modes $m > 0$ is found to become much larger than that contained in zonal flows (B). Decreasing the temperature ratio does not enable us to recover the situation observed initially - the plasma presents a phenomenon of hysteresis. When the temperature ratio is decreased, the level of energy contained in $m > 0$ remains large (C). Finally a new transition occurs (see $t2$ in Fig.2) at $T_e/T_i = 2$, where zonal flows become much stronger than instability modes (D).

We noticed that, although the qualitative shape of the hysteresis is robust, its width and height quantitatively depend on plasma parameters. For instance, the path from B to C can be shortened by reducing the maximum β (from 3.4 to 3.2 for example). We also noticed that the hysteresis effect depends very little on the time ramp of T_e/T_i. For instance there is no difference between the case $\Delta t = 5\ \omega_0^{-1}$ and the case $\Delta t = 20\ \omega_0^{-1}$ (the latter being the case considered in this paper), Δt being the time interval between each step.

It should be noted that the hysteresis effect does not depend on the radial coordinate. According to (1) and (2), $W_{m>0}$ and W_{ZF} are integrated from $\psi = 0$ to $\psi = 1$ in Fig. 2. But we obtain the same hysteresis effect if we choose to integrate over small different parts of the radial domain. Therefore, the possible non-local nature of the transport does not seem to be crucial in this case. However it should be noted that the simulation domain is quite small in our numerical experiments. Local events which can affect the global transport were not observed in the simulation box.

c. Transitions. In this paragraph we shall first focus on the transition from $T_e/T_i = 2.8$ to $T_e/T_i = 3$ ($t1$, from A to B) when the ratio increases (at $t = 200\ \omega_0^{-1}$), and next, on the second transition ($t2$, from C to D), from $T_e/T_i = 2.2$ to $T_e/T_i = 2.0$ when the ratio decreases (at $t = 400\ \omega_0^{-1}$).

We note that the transition $t1$ corresponds to a sudden change in the energy distribution between zonal flows and instabilities (Fig. 3). Although the energy of $m > 0$ modes is found to increase as a function of T_e/T_i, there is an abrupt change of slope at the transition. At the same time, zonal flows lose their intensity strongly. This transition leads to a radical change in the state of the plasma, with the confinement becoming markedly worse and the

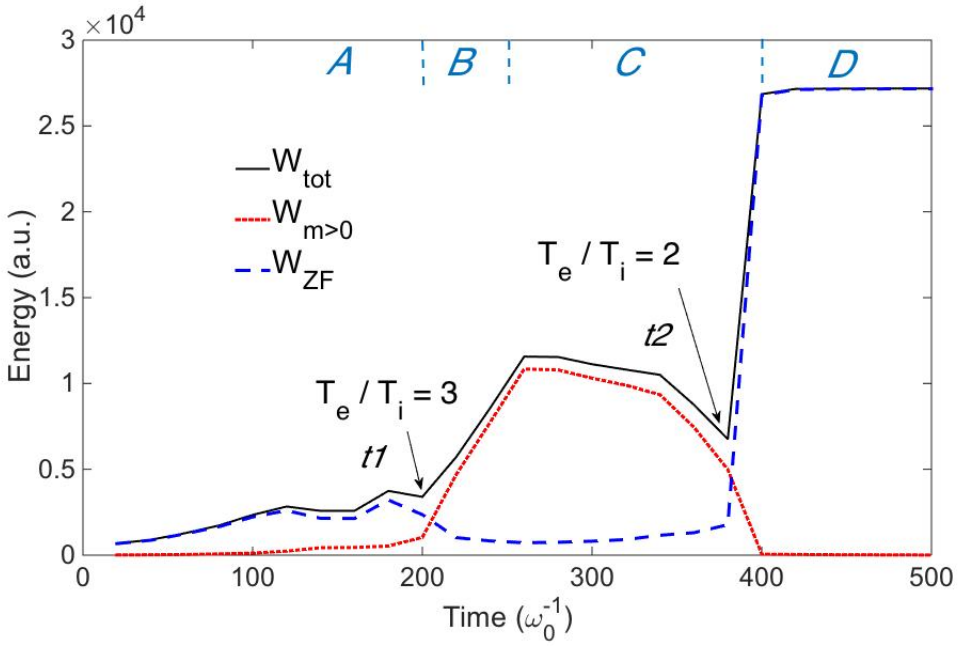

FIGURE 3. Total energy (solid curve), ZF energy (dash curve, $m = 0$) and energy contained in other modes ($m > 0$, dot curve). Starting from $T_e = T_i$, electrons are heated up to $T_e = 3.4T_i$ ($t = 250\ \omega_0^{-1}$). Next, electron temperature is decreased back down to $T_e = T_i$. Both transitions $t1$ and $t2$ discussed earlier are indicated.

radial heat transport undergoing a sharp increase. It should be noticed that this behavior can be confirmed by considering the electric potential shearing rate profile $\partial_\psi^2\phi$ as a function of ψ. The zonal flows at $t = 450.0\ \omega_0^{-1}$ are much stronger than those observed at $t = 300.0\ \omega_0^{-1}$, the shearing rate being approximately an order-of-magnitude larger. Moreover the plot of $\partial_\psi^2\phi$ as a function of time is very close to that of W_{ZF} (see Fig. 3). In this simulation experiment the energy contained in zonal flow is actually directly connected to zonal flow shear and to the turbulence suppression. Therefore a high level of improvement in energy confinement can be expected globally at the end of the hysteresis.

This transition can be studied in more detail by plotting the evolution of the modes m as a function of time, keeping in mind the relationship between time and the ratio T_e/T_i in our numerical experiment. In Fig. 4, the energy evolution of a given mode m as a function of time is shown. The power spectrum of modes plotted against time is evaluated at $\psi = 0.75$, where the strongest zonal flows are observed. It should be noticed that similar results are obtained at $\psi = 0.3$, where similar strong zonal flows are also observed. The mode $m = 0$

corresponds to the zonal flows. The other modes correspond to the instabilities. We found that at the time of the transition $t1$ (marked by a black arrow on the abscissa axis), the odd modes of the instabilities undergo an abrupt, large increase, while the even modes undergo a sharp decrease. The sharp transition therefore corresponds to a decrease in the mode $m = 0$ and a strong increase in the odd modes.

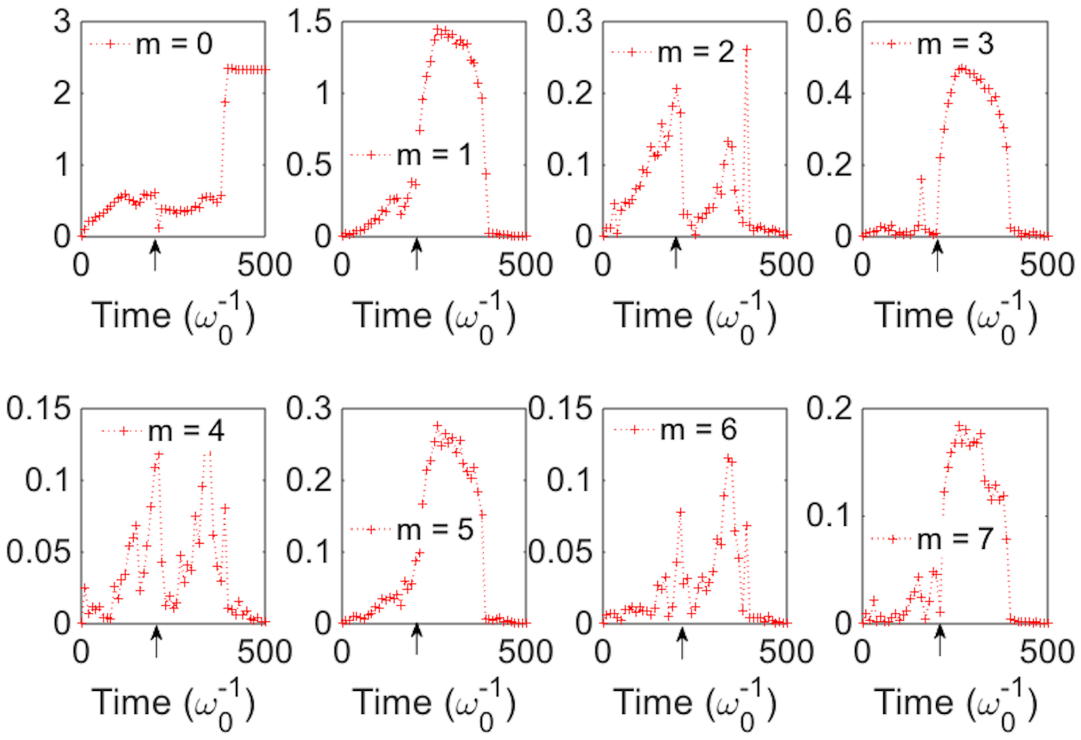

FIGURE 4. Power spectrum (a.u) of modes $m = 0$ to $m = 7$ plotted against time (which corresponds to different T_e/T_i ratios, according to Fig.1). $m = 0$ corresponds to zonal flows. The black arrow on the abscissa denotes the transition from $T_e/T_i = 2.8$ to $T_e/T_i = 3.0$ ($t1$) discussed previously. During this transition odd modes are found to dramatically increase while even modes dramatically decrease. During the other transition ($t2$), a dramatic increase of ZF ($m = 0$) is observed at $t = 400$ ω_0^{-1} while other modes drop to near zero.

Later, during the second transition $t2$, at $t = 400$ ω_0^{-1} corresponding to $T_e/T_i = 2$, the phenomenon is reversed and amplified. All the energy is found to be in the zonal flows, while the instabilities are greatly reduced and their energy becomes close to zero. When the electron temperature is the same as initially, zonal flows are found to be stronger than at the beginning of the cycle. The heat flux is found to be strongly reduced.

d. Efficiency of the control method. In a previous article [16], we showed that a control method could be applied to enhance the appearance of zonal flows while keeping the desired temperature.

In this section we proceed differently. Starting from a situation where $T_e/T_i = \beta$ (> 1), and without changing this ratio (unlike Fig.1), we observed that zonal flows occur at the beginning of the nonlinear phase but are reduced later, allowing for streamers to govern radial heat transport. We impose $T_e = T_i$ (heating is switched off), a regime where zonal flows are naturally strong and robust, before switching back to the initial $\beta > 1$ (heating is switched on again, see Fig.5) in the hope of maintaining strong and robust zonal flows.

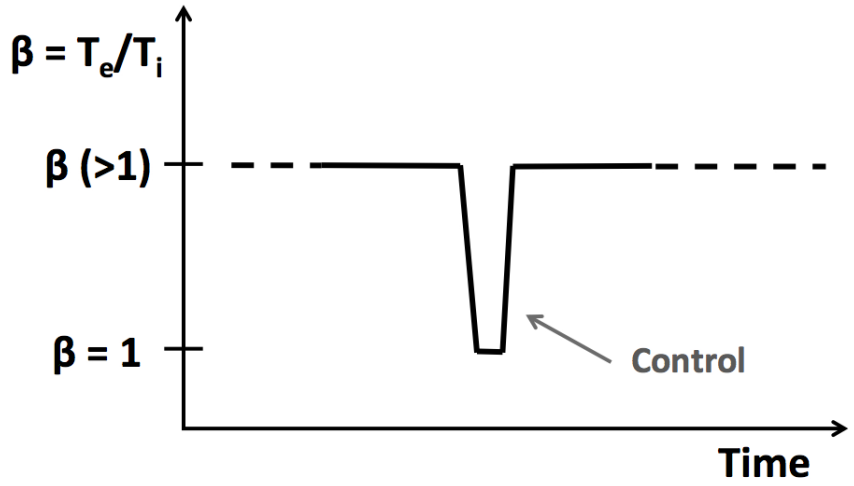

FIGURE 5. Principle of the control method described in [16].

After a short transition after the end of the control, the system was found to exhibit strong sustainable zonal flows and thus to be very effective in reducing heat fluxes. Therefore, robust and strong zonal flows are triggered by the applied control. The advantage of this method is that plasma parameters are only modified for a very short period of time without significantly modifying the performance of the plasma on the discharge time and while allowing the plasma to be heated again for long times. We found the qualitative response of the plasma to be insensitive to the duration of the control period during which we modify the plasma parameters, as both durations 0.26 ω_0^{-1} and 10 ω_0^{-1} lead to the same results for instance. Moreover, whatever the duration needed to switch the electron heating on or off (very rapid : 0.01 ω_0^{-1} or gradual : 10 ω_0^{-1}), we obtain the same results regarding the emergence of zonal flows.

However, we noticed that this method is only effective for a certain range of temperatures. The induced reduction of zonal flows is found to vary in importance (it gradually evolves) depending on the ratio T_e/T_i. For instance for $\beta = 3$, the control method appears to be inefficient. There is a link between this previous numerical experiment and the one reported in this article. We observe that this method is efficient as long as the temperature ratio is less than that of the transition $t1$. As soon as instabilities take over zonal flows - meaning as soon as they contain more energy - the method is no longer efficient and the control method is unable to durably change the dynamic state of the plasma.

Therefore the control method introduced in Ref.[16] can be interpreted as a way to take advantage of the hysteresis reported here.

e. Conclusion. We investigated the possibility of stimulating zonal flow generation and for the first time demonstrated a hysteresis phenomenon in the generation of zonal flows by using gyrokinetic simulations of core fusion plasmas. Zonal flows were driven by TEM and TIM turbulence and studied by means of gyrokinetic Vlasov simulations for trapped particles. In this work we neglected the impacts on zonal flow dynamics of 1. trapping and de-trapping processes due to turbulent/collisional pitch angle, and 2. neoclassical transport. We studied the exchange of energy between zonal flows and instabilities as a function of the electron temperature. The change in zonal flows and instabilities was found to have the characteristics of hysteresis. The plasma may have different dynamic states according to the history of the electron temperature. For the same temperature for example, the plasma may exhibit zonal flows containing different levels of energy which affects the plasma confinement. Two major transitions were observed during this hysteresis cycle - one for which instabilities suddenly develop and the other for which the zonal flows strongly take over instabilities. We have also shown that a control method used to trigger zonal flows can be considered on some parts of the cycle but is no longer effective on others.

This work was granted access to the HPC resources of IDRIS under the allocation 2017-27862 made by GENCI (Grand Equipement National de Calcul Intensif).

---

[1] Z. Lin, T. S. Hahm, W. W. Lee, W. M. Tang and R. B. White, Science 281, 1835 (1998)

[2] B. N. Rogers, W. Dorland, and M. Kotschenreuther, Phys. Rev. Lett. 85, 5336 (2000)

[3] E. Kim and P. H. Diamond, Phys. Plasmas 9, 4530 (2002)

[4] P. H. Diamond, S. I. Itoh, K. Itoh and T. S. Hahm, Plasma Phys. Control. Fusion 47, R35 (2005)

[5] Y. Asahi, A. Ishizawa, T. H. Watanabe, H. Tsutsui, S. Tsuji-lio, Phys. Plasmas 21, 052306 (2014)

[6] X. Garbet, Y. Idomura, L. Villard and T.H. Watanabe, Nucl. Fusion 50, 043002 (2010)

[7] T. Yamada *et al.*, Nature Phys. 4, 721 (2008)

[8] Z. B. Guo, T. S. Hahm, Nucl. Fusion 56, 066014 (2016)

[9] G. R. Tynan, I. Cziegler, P. H. Diamond, M. Malkov, A. Hubbard, J. W. Hugues, J. L. Terry and J. H. Irby, Nucl. Fusion 56, 066014 (2016)

[10] G. Depret, X. Garbet, P. Bertrand, A. Ghizzo, Plasma Phys. Cont. Fusion 42, 949 (2000)

[11] Y. Sarazin, V. Grandgirard, E. Fleurence, X. Garbet, Ph. Ghendrih, P. Bertrand and G. Depret, Plasma Phys. Control. Fusion 47, 1817 (2005)

[12] T. Cartier-Michaud, P. Ghendrih, Y. Sarazin, G. Dif-Pradalier, T. Drouot, D. Estève, X. Garbet, V. Grandgirard, G. Latu, C. Norscini, C. Passeron, J. Phys. : Conf. Series 561, 012003 (2014)

[13] T. Drouot, E. Gravier, T. Reveille, A. Ghizzo, P. Bertrand, X. Garbet, Y. Sarazin and T. Cartier-Michaud, Eur. Phys. Journal D 68, 280 (2014)

[14] T. Drouot, E. Gravier, T. Reveille, M. Sarrat, M. Collard, P. Bertrand, T. Cartier-Michaud, P. Ghendrih, Y. Sarazin and X. Garbet, Phys. Plasmas 22, 082302 (2015)

[15] T. Drouot, E. Gravier, T. Reveille, M. Collard, Phys. Plasmas 22, 102309 (2015)

[16] E. Gravier, M. Lesur, T. Reveille and T. Drouot, Phys. Plasmas 23, 092507 (2016)

[17] E. Sonnendrücker, J. Roche, P. Bertrand and A. Ghizzo, J. Comp. Phys. 149, 201 (1999)

[18] K.W. Gentle, M. E. Austin, J. C. DeBoo, T.C. Luce and C. C. Petty, Phys. Plasmas 13, 012311 (2006)

[19] S. Inagaki *et al.*, Nucl. Fusion 53, 113006 (2013)

[20] S. I. Itoh, K. Itoh and S. Inagaki, Nucl. Fusion 57, 022003 (2017)

[21] F. Wagner *et al.*, Phys. Rev. Lett. 49, 1408 (1982)

[22] M. A. Malkov and P. H. Diamond, Phys. Plasmas 23, 16012504 (2009)

[23] C. S. Chang, S. Ku, G. R. Tynan *et al.*, Phys. Rev. Lett. 118, 175001 (2017)